

Properties of Mn-doped Cu₂O semiconducting thin films grown by pulsed-laser deposition

M. Ivill^{a,*}, M.E. Overberg^a, C.R. Abernathy^a, D.P. Norton^a,
A.F. Hebard^b, N. Theodoropoulou^b, J.D. Budai^c

^a Department of Materials Science and Engineering, University of Florida, Gainesville, FL 32611-8440, USA

^b Department of Physics, University of Florida, Gainesville, FL 32611-8440, USA

^c Oak Ridge National Laboratory, Oak Ridge, TN 37831, USA

Received 17 January 2003; received in revised form 21 February 2003; accepted 9 April 2003

Abstract

Semiconducting oxides offer the potential for exploring and understanding spin-based functionality in a semiconducting host material. Theoretical predictions suggest that carrier-mediated ferromagnetism should be favored for p-type material. Cu₂O is a p-type, direct wide bandgap oxide semiconductor that may hold interest in exploring spin behavior. In this paper, the properties of Mn-doped Cu₂O are described. Activities focused on understanding Mn incorporation during thin-film synthesis, as well as magnetic characterization. The epitaxial films were grown by pulsed-laser deposition. X-ray diffraction was used to determine film crystallinity and to address the formation of secondary phases. SQUID magnetometry was employed to characterize the magnetic properties. Ferromagnetism is observed in selected Mn-doped Cu₂O films, but appears to be associated with Mn₃O₄ secondary phases. In phase-pure Mn-doped Cu₂O films, no evidence for ferromagnetism is observed.

© 2003 Elsevier Ltd. All rights reserved.

1. Introduction

The study of transition metal doped semiconducting material is useful in understanding and developing spintronic concepts. In recent years, the injection and manipulation of spin-polarized electrons in semiconductor materials has become the focus of intense research activity [1,2]. A functional spin offers an opportunity to develop new device concepts based on the discrimination and manipulation of spin distributions. Fundamental challenges related to the lifetime, manipulation, and detection of spin-polarized electrons in a semiconductor host must be addressed in order to realize spintronic technology based on semiconductors. Of particular importance is the realization of spin-polarized currents in a semiconductor matrix. Recent experiments indicate that

injection of spin-polarized electrons from a ferromagnetic semiconductor into a non-ferromagnetic semiconductor is possible without detrimental interface scattering. Unfortunately, ferromagnetism in semiconductors is rare and poorly understood, with ferromagnetic transition temperatures well below room temperature for most known materials.

Magnetism in semiconductor materials has been studied for many years, and includes spin glass and antiferromagnetic behavior in Mn-doped II–VI compounds, as well as ferromagnetism in europium chalcogenides and Cr-based spinels [3–5]. In recent years, ferromagnetism in semiconductors, including oxides, has received renewed attention, partly due to interest in spintronic device concepts [1,6–9]. Due to transition metal solubility and technological interest, contemporary research has primarily focused on II–VI and III–V materials. Strong ferromagnetic interaction between localized spins has been observed in Mn-doped II–VI compounds with high carrier densities. In Pb_{1-x-y}Sn_yMn_xTe ($y > 0.6$) possessing a hole concentration on the

* Corresponding author. Tel.: +1-352-846-1091; fax: +1-352-846-1182.

E-mail address: mivil@mse.ufl.edu (M. Ivill).

order of 10^{20} – 10^{21} cm^{-3} , ferromagnetism has been achieved [10]. In addition, it has been shown that free holes in low-dimensional structures of II–VI dilute magnetic semiconductors can induce ferromagnetic order [11]. For many semiconductor materials, the bulk solid solubility for magnetic and/or electronic dopants is not conducive with the coexistence of carriers and spins in high densities. However, the low solubility for transition metals in semiconductors can often be overcome via low temperature epitaxial growth. This approach has been used with Mn-doped GaAs [12] in achieving ferromagnetism with a transition temperature of 110 K, which is remarkably high compared to traditional dilute magnetic semiconductor material. Behavior indicative of ferromagnetism at temperatures above 300 K has recently been reported for GaN and chalcopyrite semiconductors doped with transition metals, illustrating the potential of achieving room temperature spintronics technologies [13,14].

Despite recent experimental success, a fundamental description of ferromagnetism in semiconductors remains incomplete. Recent theoretical treatments have yielded useful insight into fundamental mechanisms [15]. Dietl et al. have applied Zener's model for ferromagnetism, driven by exchange interaction between carriers and localized spins, to explain the ferromagnetic transition temperature in III–V and II–VI compound semiconductors. The theory assumes ferromagnetic correlations mediated by holes from shallow acceptors in a matrix of localized spins in a magnetically doped semiconductor. Specifically, Mn ions substituted on the group II or III site provide the local spin. In the case of III–V semiconductors, Mn also provides the acceptor dopant. High concentrations of holes are believed to mediate the ferromagnetic interactions among Mn ions. Direct exchange among Mn is antiferromagnetic as observed in fully compensated (Ga,Mn)As that is donor-doped. In the case of electron doped or heavily Mn-doped materials, no ferromagnetism is detected. Theoretical results suggest that carrier-mediated ferromagnetism in n-type material should be relegated to low temperatures, if it occurs at all, while it is predicted at higher temperatures for p-type materials [16]. In p-type GaAs grown by low temperature MBE, Mn doping in the concentration range $0.04 \leq x \leq 0.06$ results in ferromagnetism in GaAs. The model described has been reasonably successful in explaining the relatively high transition temperature observed for (Ga,Mn)As.

Carrier-mediated ferromagnetism in semiconductors is dependent on the magnetic dopant concentration as well as on the carrier type and carrier density. As these systems can be envisioned as approaching a metal–insulator transition when carrier density is increased and ferromagnetism is observed, it is useful to consider the effect of localization on the onset of ferromagnetism. As carrier density is increased, the progression from

localized states to itinerant electrons is gradual. On the metallic side of the transition, some electrons populate extended states while others reside at singly occupied impurity states. On crossing the metal–insulator boundary, the extended states become localized, although the localization radius gradually decreases from infinity. For interactions on a length scale smaller than the localization length, the electron wavefunction remains extended. In theory, holes in extended or weakly localized states could mediate the long-range interactions between localized spins. This suggests that for materials that are marginally localized, such as in low mobility semiconducting oxides, carrier-mediated ferromagnetic interactions may be possible.

In this paper, the synthesis and properties of Mn-doped Cu_2O epitaxial thin films is described. Cu_2O is one of the few binary p-type semiconducting oxides, possessing a direct bandgap of 2.0 eV and a reasonably high room temperature hole mobility of $\sim 100 \text{ cm}^2 \text{ v}^{-1} \text{ s}^{-1}$ [17]. The structure is cubic, with $a = 4.27 \text{ \AA}$. In Cu_2O , p-type conductivity is due to copper vacancies introducing an acceptor level ~ 0.5 eV above the valence band. For the materials that have been theoretically considered in detail (semiconductors with zinc-blende structure), magnetic interactions are favored in hole-doped materials due to the interaction of Mn^{2+} ions with the valence band. This is consistent with previous calculations for the exchange interaction between Mn^{2+} ions in II–VI compounds, [3] showing that the dominant contribution is from two-hole processes. This superexchange mechanism can be viewed as an indirect exchange interaction mediated by the anions, thus involving the valence band. The present study focuses on Mn-doped p-type Cu_2O films.

2. Experimental description

Pulsed-laser deposition was used for film growth. Manganese-doped CuO targets were fabricated using high-purity CuO (99.995%), with MnO_2 (99.999%) serving as the doping agent. The targets were pressed and sintered at 860 °C for 12 h, followed by 950 °C for 2 h in air. Targets were fabricated with a composition of $\text{Cu}_{1.9}\text{Mn}_{0.1}\text{O}$. A KrF excimer laser was used as the ablation source. A laser repetition rate of 5 Hz was used, with a target to substrate distance of 4 cm and a laser pulse energy density of 1–3 J/cm^2 . The growth chamber exhibits a base pressure of 10^{-6} Torr. Film thickness was approximately 300 nm. Single crystal (001) MgAl_2O_3 and MgO were used as the substrate material in this study. Four-circle X-ray diffraction was used to determine crystallinity and dopant solubility. SQUID magnetometry was used to characterize the magnetic properties of the deposited films. In particular, it was used to determine the presence of ferromagnetism and measure the

Curie temperature. Photoluminescence was used to characterize the optical properties of the material.

3. Results and discussion

The epitaxial growth of Cu_2O thin films is dependent upon achieving oxidation conditions in which the Cu ion assumes a 1+ valence. Fig. 1 shows the thermodynamic stability curves for Cu– Cu_2O –CuO as a function of oxygen partial pressure and temperature [18]. Using this, we find that epitaxial Cu_2O films can be grown from high-purity CuO or Cu targets using pulsed-laser deposition in an oxygen ambient. Fig. 2 shows the X-ray diffraction data for a (001) Cu_2O film grown on (001) MgO with $P(\text{O}_2) = 4 \times 10^{-4}$ Torr, $T = 750$ °C, using a Cu target. Similar results were obtained on perovskite substrates, yielding p-type films with a carrier density of $\sim 10^{15}$ cm^{-3} and a room temperature mobility of 26 $\text{cm}^2 \text{v}^{-1} \text{s}^{-1}$. The primary focus of this work was to investigate the synthesis and properties of epitaxial Cu_2O

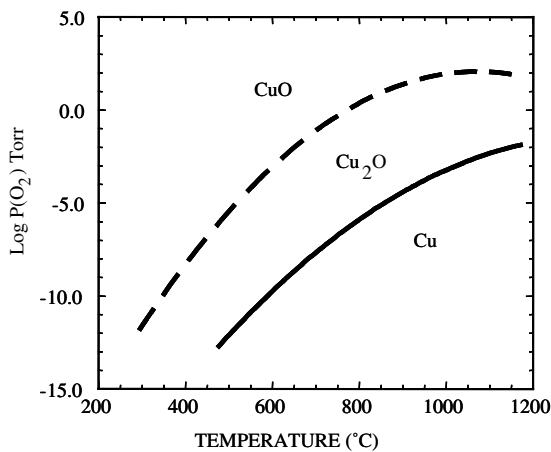


Fig. 1. Phase stability curves for the Cu– Cu_2O –CuO system.

doped with Mn. The selection of Mn as the transition metal dopants is based on the best available evidence in determining which magnetic impurities are likely to yield ferromagnetism. Manganese doping has resulted in interesting magnetic phenomenon in II–VI and III–V semiconductors, including spin glass or antiferromagnetic behavior for a number of systems, and is predicted to yield a high Curie temperature in ZnO as previously discussed. In the Cu_2O structure, the Cu^{1+} cation is twofold coordinated with an ionic radius of 0.46 Å. Mn^{2+} does not normally exhibit a twofold coordination in bulk materials. However, the radius for fourfold coordinated Mn^{2+} is 0.66 Å, which is close to that for the fourfold coordinated Cu^{1+} (0.60 Å). As a 2+ cation on a 1+ site, Mn would be expected to compensate for the p-type conductivity observed in Cu_2O . The resistivity of Mn-doped Cu_2O films was significantly higher than that for undoped films.

The phase stability and solid solubility of Mn in Cu_2O was investigated as a function of deposition temperature and oxygen pressure. X-ray diffraction was used to determine conditions that limit segregation of secondary phases. Film growth was carried out over a temperature range of 300–700 °C and an oxygen pressure of 10^{-3} , 10^{-4} Torr, or in vacuum. The base pressure of 10^{-5} Torr consists mostly of water vapor. Figs. 3–5 shows the X-ray diffraction data for Mn-doped films grown under these conditions. Several items should be noted. First, the Cu_2O phase is dominant over most of this range. This is surprising as the thermodynamic stability behavior suggests that CuO should be the stable phase for $T < 600$ °C, $P(\text{O}_2) = 10^{-3}$ Torr, and $T < 550$ °C, $P(\text{O}_2) = 10^{-4}$ Torr. Two possibilities exist in explaining this discrepancy. First, the doping of Cu_2O with Mn may shift the phase stability line. Second, epitaxy at low temperature may be sufficient to stabilize the Cu_2O phase. A segregation of Mn oxides in the Mn-doped films was also examined for the various film-growth conditions. The X-ray diffraction results indicate the presence of antiferromagnetic Mn_2O_3 as an impurity

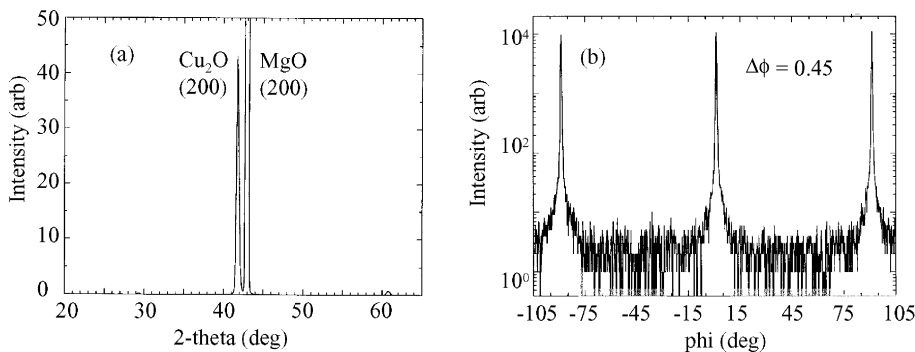


Fig. 2. X-ray diffraction data for epitaxial Cu_2O on (001) MgO, showing both (a) out-of-plane and (b) in-plane orientation.

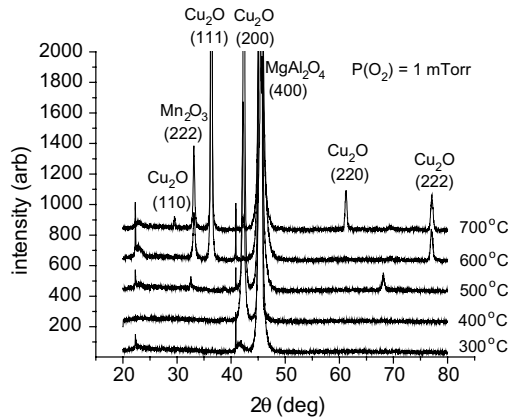


Fig. 3. X-ray diffraction data for Mn-doped Cu_2O films grown on (001) MgAl_2O_4 in an oxygen pressure of 1 mTorr.

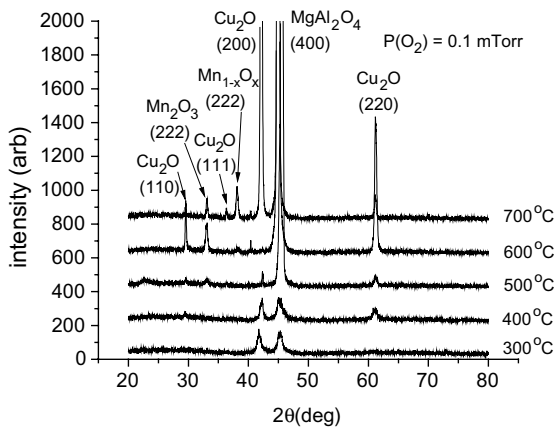


Fig. 4. X-ray diffraction data for Mn-doped Cu_2O films grown on (001) MgAl_2O_4 in an oxygen pressure of 0.1 mTorr.

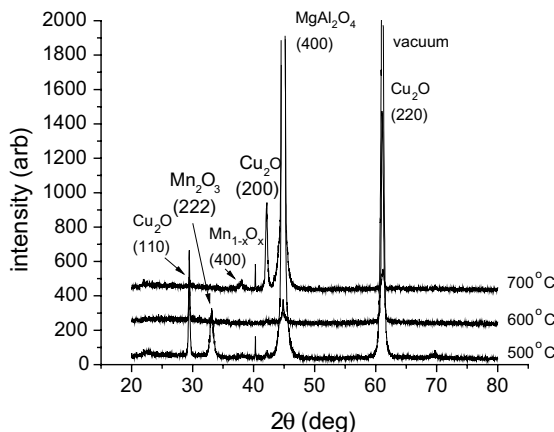


Fig. 5. X-ray diffraction data for Mn-doped Cu_2O films grown on (001) MgAl_2O_4 in vacuum.

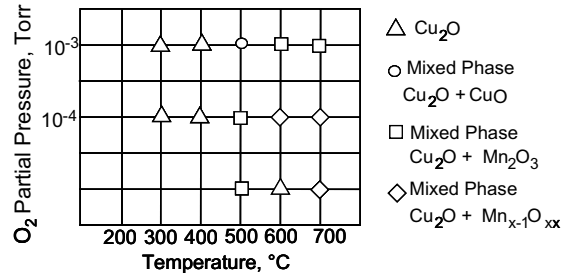


Fig. 6. Phase assemblage for films grown under different conditions.

phase for $T \geq 500$ °C. For films grown in vacuum, a weak peak that could be associated with either Mn_2O_3 or ferromagnetic Mn_3O_4 is observed. Phase-pure Cu_2O films were obtained at $T \leq 400$ °C, indicating the metastable incorporation of Mn in the Cu_2O matrix. Fig. 6 shows the phase assemblage as a function of growth conditions.

The magnetic properties of Mn-doped samples were measured using a Quantum Design SQUID magnetometer. Measurements were made on films grown at low temperatures, in which no Mn_3O_4 impurity phase peaks were evident in the X-ray diffraction patterns, as well as films grown at elevated temperatures. In order to characterize the magnetic properties of the Mn-doped samples, field-cooled and zero field-cooled magnetization measurements were performed from 4.2 to 300 K. By taking the difference (ΔM) between these two quantities, the para- and diamagnetic contributions to the magnetization can be subtracted, leaving only a measure of ferromagnetic behavior. Fig. 7 shows the ΔM difference as a function of temperature for a Mn-doped sample grown at 300 °C in 1 m Torr of O_2 . At low temperature, a small, but finite field-cooled minus zero field-cooled magnetic signal persists up to ~ 250 K as seen in Fig. 7. However, the magnetization signal is small, and can be attributed to a background magnetic signal from the MgAl_2O_4 substrate. Fig. 8 shows the temperature dependent ΔM and M vs. H behavior for the substrate material without a Cu_2O film. For this and other phase-pure samples, no ferromagnetism could be detected about that attributed to the substrate.

We also investigated the magnetic properties of Mn-doped Cu_2O grown at 700 °C. These epitaxial Mn-doped Cu_2O films are clearly ferromagnetic with a T_c of ~ 48 K as seen in Fig. 9. A key requirement in understanding ferromagnetism in transition metal doped semiconductors is to delineate whether the magnetism originates from substitutional dopants on cation sites, or from the formation of a secondary phase that is ferromagnetic. The importance of this issue cannot be understated. The concept of spintronics based on ferromagnetic semiconductors assumes that the spin polarization exists in the distribution of semiconductor carriers. Localized

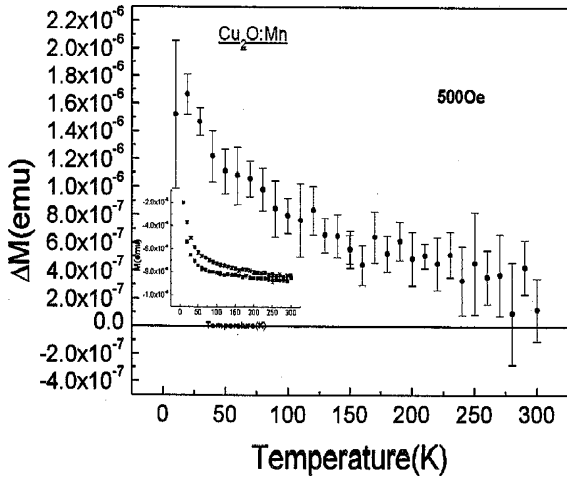


Fig. 7. Magnetic behavior for an epitaxial Mn-doped Cu_2O film grown at 300 °C and 1 mTorr of oxygen.

magnetic precipitates might be of interest in nanomagnetism, but is of little utility for semiconductor-based spintronics. The question of precipitates vs. carrier-mediated ferromagnetism is complex, and is a central

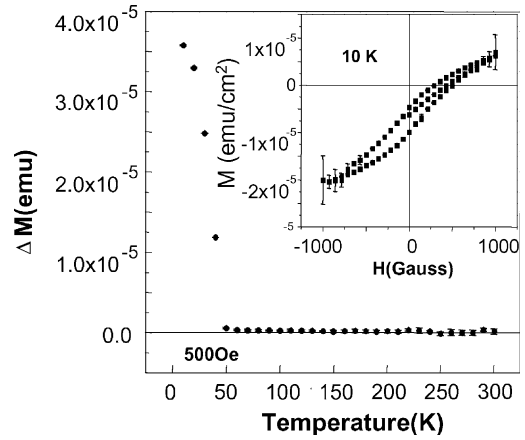


Fig. 9. Magnetic behavior for an epitaxial Mn-doped Cu_2O film grown at 700 °C in vacuum.

topic of discussion for other semiconducting oxides that exhibit ferromagnetism, in particular the Co-doped TiO_2 system [19,20]. Several issues must be addressed in order to gain insight into the possible role of secondary phase precipitates in the magnetic properties of transition

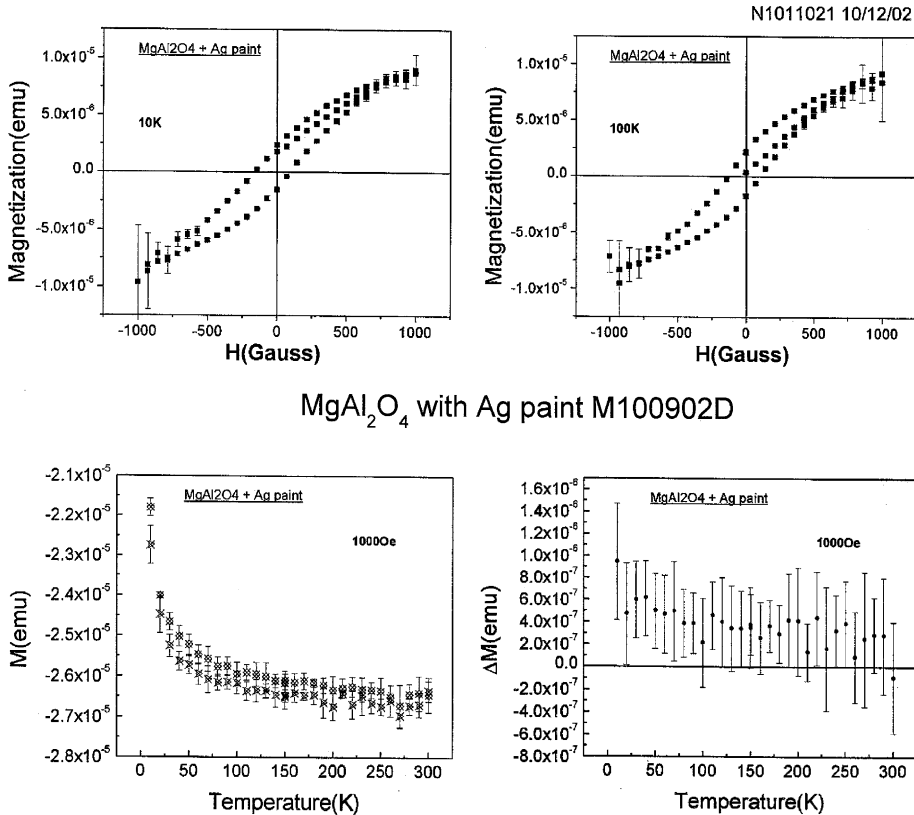


Fig. 8. Magnetic behavior for MgAl_2O_4 substrate.

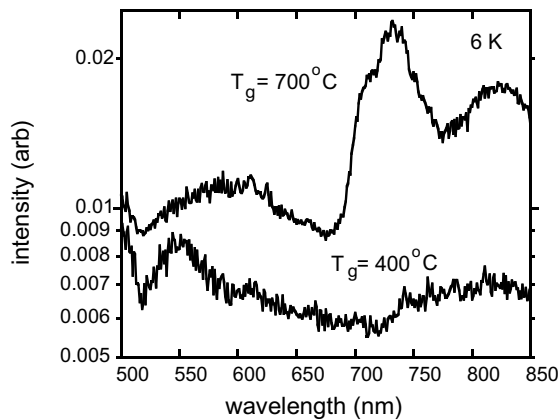


Fig. 10. Low temperature photoluminescence spectra for Mn-doped Cu_2O films.

metal doped semiconductors, specifically for Cu_2O films. First, one should identify all candidate magnetic phases possible from the assemblage of elements. The coincidence of T_c with a known candidate secondary ferromagnetic phase indicates a likely source of at least part of the magnetic signature. For the present material, metallic Mn is antiferromagnetic, with a Néel temperature of 100 K. In addition, nearly all of the possible Mn-based binary and ternary oxide candidates are antiferromagnetic. The exception to this is Mn_3O_4 , which is ferromagnetic with a Curie temperature of 46 K [21,22]. X-ray diffraction measurements on the sample considered in Fig. 9 show evidence for the Mn_3O_4 phase. Obviously, the simplest explanation for ferromagnetic behavior in this material is Mn_3O_4 precipitates.

In addition to magnetization, the optical properties were also examined. The photoluminescence properties of the films were measured at room temperature using a He–Cd laser (325 nm) and taken over a wavelength range of 350–800 nm. The power density was 1 W/cm^2 . A 0.3 m scanning grating monochromator with a Peltier-cooled GaAs photomultiplier was utilized. The plot in Fig. 10 shows photoluminescence spectra for Mn-doped Cu_2O films deposited at 400 and 700 °C. The peak at 610 nm corresponds to the 1 s exciton [23–25]. This peak is rather weak and broad, but is most evident in the film grown at 700 °C. Note also the peak at $\sim 735 \text{ nm}$, which has previously been associated with extrinsic defects in the Cu_2O material [26]. Most of the additional broad peaks could be attributed to the background photoluminescence from the substrate. The emergence of intrinsic photoluminescence in the film grown at 700 °C is consistent with the segregation of Mn from the Cu_2O matrix. It is also possible that luminescence from either Mn^{2+} or Mn^{4+} also contributes to the spectra observed.

Acknowledgements

This research was partially sponsored by the Army Research Office under grant no. DAAD19-01-1-0603. The authors would also like to acknowledge the Major Analytical Instrumentation Center, Department of Materials Science and Engineering, University of Florida.

References

- [1] Wolf SA. *J Supercond* 2000;13:195.
- [2] Prinz GA. *Science* 1998;282:1660.
- [3] Furdyna JK. *J Appl Phys* 1988;64:R29.
- [4] Gopalan S, Cottam MG. *Phys Rev B* 1990;42:10311.
- [5] Haas C. *Crit Rev Solid State Sci* 1970;1:47.
- [6] Sato K, Katayama-Yoshida H. *Jpn J Appl Phys* 2000;39:L555.
- [7] Wakano T, Fujimura N, Morinaga Y, Abe N, Ashida A, Ito T. *Physica C* 2001;10:260.
- [8] Fukumura T, Jin Z, Ohtomo A, Koinuma H, Kawasaki M. *Appl Phys Lett* 1999;75:3366.
- [9] Jung SW, An S-J, Yi G-C, Jung CU, Lee S-I, Cho S. *Appl Phys Lett* 2002;80:4561.
- [10] Suski T, Igalson J, Story T. *J Magn Magn Mater* 1987;66:325.
- [11] Hauray A, Wasiela A, Arnoult A, Cibert J, Tatarenko S, Dietl T, et al. *Phys Rev Lett* 1997;79:511; Kossacki P, Ferrand D, Arnoult A, Cibert J, Tatarenko S, Wasiela A, et al. *Physica E* 2000;6:709.
- [12] Ohno H. *Science* 1998;281:951.
- [13] Sato K, Medvedkin GA, Nishi T, Hasegawa Y, Misawa R, Hirose K, et al. *J Appl Phys* 2001;89:7027.
- [14] Overberg ME, Gila BP, Thaler GT, Abernathy CR, Pearton SJ, Theodoropoulou NA, et al. *J Vac Sci Technol B (Microelectron Nanometer Struct)* 2002;20:969.
- [15] Dietl T, Ohno H, Matsukura F, Cubert J, Ferrand D. *Science* 2000;287:1019.
- [16] Dietl T, Hauray A, Merle d'Aubigne Y. *Phys Rev B* 1997;55:R3347.
- [17] Young AP, Schwartz CM. *J Phys Chem Solids* 1969;30:249.
- [18] Rakhshani AE. *Solid-State Electron* 1986;29:7.
- [19] Matsumoto Y, Murakami M, Shono T, Hasegawa T, Fukumura T, Kawasaki M, et al. *Science* 2001;291:854.
- [20] Chambers SA, Thevuthasan S, Farrow RFC, Marks RF, Thiele UU, Folks L, et al. *Appl Phys Lett* 2001;79:3467.
- [21] Guo LW, Peng DL, Makino H, Inaba K, Ko HJ, Sumiyama K, et al. *J Magn Magn Mater* 2000;213:321.
- [22] Chartier A, D'Arco P, Dovesi R, Saunders VR. *Phys Rev B (Cond Mat)* 1999;60:14042.
- [23] Petroff Y, Yu PY, Shen YR. *Phys Rev B* 1975;12:2488.
- [24] Sun Y, Rivkin K, Chen J, Ketterson JB, Markworth P, Chang RP. *Phys Rev B* 2002;66:245315.
- [25] Ito T, Yamaguchi H, Okabe K, Masumi T. *J Mater Sci* 1998;33:3555.
- [26] Kenway DJ, Duvvury C, Weichman FL. *J Lumin* 1978;16:171.